

# Clustering of the Diffuse Infrared Light from the COBE DIRBE maps. An all-sky survey of $C(0)$ .

A. Kashlinsky<sup>1</sup>, J. C. Mather<sup>2</sup>, S. Odenwald<sup>3</sup>

<sup>1</sup>NORDITA, Blegdamsvej 17, DK-2100 Copenhagen, Denmark

<sup>2</sup>Code 685, NASA Goddard Space Flight Center, Greenbelt, MD 20771

<sup>3</sup>Hughes STX Corporation, Code 685.3,

NASA Goddard Space Flight Center, Greenbelt, MD 20771

Received \_\_\_\_\_; accepted \_\_\_\_\_

## ABSTRACT

We measure the smoothness of the infrared sky using the COBE DIRBE maps, and obtain interesting limits on the production of the diffuse cosmic infrared background (CIB) light by matter clustered like galaxies. The predicted fluctuations of the CIB with the DIRBE beam size of  $0.7^\circ$  are of the order of 10%, and the maps are smooth at the level of  $\delta\nu I_\nu \sim$  a few  $\text{nWm}^{-2}\text{sr}^{-1}$  rms from 2.2 to  $100 \mu\text{m}$ . The lowest numbers are achieved at mid- to far-IR where the foreground is bright but smooth; they are  $\sqrt{C(0)} \leq (1 - 1.5) \text{ nWm}^{-2}\text{sr}^{-1}$  at  $\lambda = 10\text{-}100 \mu\text{m}$ . If the CIB comes from clustered matter evolving according to typical scenarios, then the smoothness of the maps implies CIB levels less than  $\sim (10 - 15) \text{ nWm}^{-2}\text{sr}^{-1}$  over this wavelength range.

*Subject headings:* Cosmology: Theory – Cosmology: Observations – Diffuse Radiation – Large Scale Structure of the Universe – Galaxies: Evolution

## 1. Introduction

The cosmic infrared background (CIB) contains information about the conditions in the post-recombination Universe and links the microwave background, which probes the last scattering surface, and the optical part of the cosmic spectrum, which probes the conditions in the Universe today at  $z \sim 0$ . Numerous models have been developed to predict the properties of the CIB at wavelengths from the near-IR ( $\lambda \sim 1\text{-}10 \mu\text{m}$ ) to the far-IR (e.g. Bond, Carr and Hogan 1986; Beichman and Helou 1991; Franceschini *et al.* 1991). The predicted spectral properties and the amplitude of the CIB depend on the various cosmological assumptions used, such as the cosmological density parameter, the history of star formation, and the power spectrum of the primordial density field among others. A typical prediction over the range of wavelengths probed by the COBE (Cosmic Background Explorer) DIRBE (Diffuse Infrared Background Experiment),  $1.25 - 240 \mu\text{m}$ , is  $\nu I_\nu \sim 10 \text{ nW m}^{-2} \text{sr}^{-1}$  (e.g. Pagel 1993 and references therein). It is difficult to measure such levels directly because the foreground emissions from stars and interstellar and interplanetary dust are bright.

An alternative to direct photometric measurements of the uniform (DC) component of the CIB is to study its spatial structure. In such a method, the groundwork for which has been laid in Kashlinsky, Mather, Odenwald and Hauser (1996; hereafter Paper I), one compares the predicted fluctuations of the CIB with the measured angular correlation function of the maps. Here we apply the method to the all-sky DIRBE maps and show that it imposes interesting limits on the CIB from clustered matter, particularly in the mid- to far-IR. We review the theoretical basis for the analysis and improve it over Paper I, discuss the data sets and the methods of map construction and analysis, and conclude with the results and limits they set on the CIB.

## 2. Theory

The angular correlation function for the CIB has been studied for a variety of cosmological models (e.g. Bond, Carr and Hogan 1986, Wang 1991, Coles, Treyer and Silk 1990, Paper I). In general, the intrinsic correlation function of the diffuse background,  $C(\theta) \equiv \langle \nu \delta I_\nu(\mathbf{x}) \cdot \nu \delta I_\nu(\mathbf{x} + \theta) \rangle$ , where  $\delta I \equiv I - \langle I \rangle$  is the map of spatial fluctuations produced by a population of emitters (e.g. galaxies) clustered with a 3-dimensional correlation function  $\xi(r)$ , is given in the small angle limit ( $\theta \ll 1$ ) by

$$C(\theta) = \int_0^\infty A_\theta(z) \left( \frac{d\nu I_\nu}{dz} \right)^2 [\Psi^2(z)(1+z)^2 \sqrt{1+\Omega z}] dz, \quad (1)$$

where it was assumed that the cosmological constant is zero,  $\Psi(z)$  is the factor accounting for the evolution of the clustering pattern, and  $A_\theta(z) = 2R_H^{-1} \int_0^\infty \xi(\sqrt{v^2 + \frac{x^2(z)\theta^2}{(1+z)^2}}) dv$ . Here  $R_H = cH_0^{-1}$ , and  $x(z)$  is the comoving distance. In case of non-zero cosmological constant,  $\Lambda \equiv 3H_0^2\lambda$ , the  $\sqrt{1+\Omega z}$  term in the parentheses above should be replaced with  $\sqrt{1+\Omega z + \lambda[(1+z)^{-2} - 1]}$ . After convolving Eq. 1 with the beam, the zero-lag correlation function (mean square deviation) becomes

$$C_\vartheta(0) = \int_0^\infty A_\vartheta(z) \left( \frac{d\nu I_\nu}{dz} \right)^2 [\Psi^2(1+z)^2 \sqrt{1+\Omega z}] dz, \quad (2)$$

$$A_\vartheta(z) = \frac{1}{2\pi R_H} \int_0^\infty P_{3,0}(k) k W\left(\frac{kx(z)\vartheta}{1+z}\right) dk. \quad (3)$$

For the top-hat beam of DIRBE the window function is  $W(x) = [2J_1(x)/x]^2$  and  $\vartheta=0.46^\circ$ . In Eq. 3,  $P_{3,0}(k)$  is the spectrum of galaxy clustering at the present epoch. If  $\xi$  is known, the measurement of  $C(\theta)$  can give information on the diffuse background due to material clustered like galaxies (e.g. Gunn 1965, Peebles 1980). Such a method was successfully applied in the V (Shectman 1973, 1974) and UV bands (Martin and Bowyer 1989). In the rest of the paper we omit the subscript  $\vartheta$  in Eq. 3, with  $C(0)$  referring to the DIRBE convolved zero-lag correlation signal; the mean square of the map  $\langle (\nu \delta I_\nu)^2 \rangle$ . This  $C(0)$  is just the mean square confusion noise.

As was shown in Paper I, for scales dominating the integral in Eq. 2 the 2-point correlation function at the present epoch can be approximated as a power-law. In that case, in the Friedman-Robertson-Walker Universe,  $A_\vartheta(z)$  would reach a minimum at  $z \geq 1$  whose value is almost independent of  $\Omega$ . Here we generalize the argument to a more realistic  $\xi(r)$ . We computed  $A_\vartheta(z)$  using the correlation data from the APM (Maddox *et al.* 1990) survey, with the APM power spectrum taken from: 1) the inversion technique of Baugh and Efstathiou (1993; hereafter BE), and; 2) the empirical fit to the APM data on the projected galaxy correlation function from Kashlinsky (1992; hereafter K92). The resultant  $A_\vartheta(z)$  is shown in Fig. 1 for  $\Omega=1$  (upper sets of lines) and 0.1 (lower sets). The solid lines correspond to BE and the dashed lines to K92 spectra  $P_{3,0}(k)$ . Both were normalized to the Harrison-Zeldovich spectrum at wavenumbers smaller than those probed by the APM data, as required by the COBE/DMR observations (Bennett *et al.* 1996). The three sets of curves for each  $\Omega$  indicate the  $1\sigma$  uncertainty from the APM data from the BE inversion and a roughly similar uncertainty from the K92 empirical fit. The minimum of  $A_\vartheta(z)$  is clear, and for the scales probed by the DIRBE beam the value at the minimum is practically independent of  $\Omega$ . Following Paper I we can rewrite Eq. 2 as an inequality to derive an upper limit on a measure of the CIB flux from clustered material from any upper limit on  $C(0)$  derived from the DIRBE data:

$$(\nu I_\nu)_{z,rms} \leq B \sqrt{C(0)} \quad (4)$$

where  $B \equiv 1/\sqrt{\min\{A_\vartheta(z)\}} = (11-14)$  over the entire range of parameters, and the measure of the CIB flux used in Eq. 4 is defined as  $[(\nu I_\nu)_{z,rms}]^2 \equiv \int (\frac{d\nu I_\nu}{dz})^2 [\Psi^2(z)(1+z)^2 \sqrt{1+\Omega z}] dz$ . The latter is  $\simeq \int (\frac{d\nu I_\nu}{dz})^2 dz$  since the term in the brackets has little variation with  $z$  for two extremes of clustering evolution, when it is stable in either proper or comoving coordinates (Peebles 1980). Thus the CIB produced by objects clustered like galaxies should have significant fluctuations,  $\sim 10\%$  of the total flux, on the angular scale subtended by the DIRBE beam. As Eq. 2 shows, if the bulk of the CIB comes from higher redshifts this

would lead to smaller relative  $\delta I/I$  and vice versa (cf. Wang 1991).

### 3. Data and analysis

The COBE was launched in 1989 (Boggess *et al.* 1992). The DIRBE is one of the three instruments, and mapped the sky in ten bands from the near-IR (J, K, L bands at  $\lambda=1.25$ , 2.2 and 3.5  $\mu\text{m}$ ) to the far-IR at 240  $\mu\text{m}$ . Four of the bands match the IRAS bands. The instrument is a photometer with an instantaneous field of view of  $0.7^\circ \times 0.7^\circ$ . It was designed to have a mission-averaged, instrumental noise less than  $1 \text{ nWm}^{-2}\text{sr}^{-1}$  in the first eight bands; at 140 and 240  $\mu\text{m}$  the instrumental noise is higher.

We analyzed maps for all 10 DIRBE bands derived from the entire 41 week DIRBE data set available from the NSSDC. A parametrized model developed by the DIRBE team (Reach *et al.* 1996) was used to remove the time-varying zodiacal component from each weekly map (Paper I). The maps were pixelized using the quadrilateralized spherical cube as described by Chan and O'Neill (1974) and Chan and Laubscher (1976).

After the maps were constructed, the sky was divided into 384 patches of  $32 \times 32$  pixels  $\simeq 10^\circ \times 10^\circ$  each. Each field was cleaned of bright sources by the program developed by the DIRBE team, in which the large scale flux distribution in each patch was modeled with a fourth order polynomial. As in Paper I, pixels with fluxes  $> N_{\text{cut}}$  standard deviations above the fitted model were removed along with the surrounding 8 pixels. Three values of  $N_{\text{cut}}$  were used:  $N_{\text{cut}} = 7, 5, 3.5$ . Since any large-scale gradients in the emission are clearly due to the local foregrounds, a fourth order polynomial was also removed from each patch after desourcing. The extragalactic contribution to  $C(0)$  should come predominantly from small scales, so removing large scale gradients would not remove any significant part of the extragalactic  $C(0)$ . In any case, we confirmed that removing the local gradients with lower

order polynomials makes little difference in the final results. We also verified that there is a good correlation between removed bright objects in the 1.25, 2.2, and 3.5  $\mu\text{m}$  bands at  $N_{\text{cut}} = 7$  and the stars from the SAO catalog; at lower  $N_{\text{cut}}$  many of the removed peaks would be too dim to enter the catalog.

The results of the calculations of  $C(0)$  for all 384 patches at  $N_{\text{cut}} = 3.5$  for wavelengths from 1.25 to 100  $\mu\text{m}$  are shown in Plate 1 in Galactic coordinates. Sixteen shades are used with a logarithmic increment of  $\simeq 1.8$  in  $C(0)$  starting at the minimal values in each band. The fluctuations in all bands are strongest where the foregrounds are brightest in the Galactic or Ecliptic plane. The histograms for the  $C(0)$  maps in each band show that the range of values for  $C(0)$  are very different in the near-IR (1.25 - 4.9  $\mu\text{m}$ ) and mid- to far-IR (12-100  $\mu\text{m}$ ) bands. In the near-IR where Galactic stars dominate the fluctuations of the foreground, there is the expected dependence of the minimal value of  $C(0)$  on the desourcng parameter  $N_{\text{cut}}$ . At mid- to far-IR there is very little change in the distribution of  $C(0)$  with  $N_{\text{cut}}$  since the foreground emission is extended with little small-scale structure.

In the near-IR bands where Galactic stars dominate the foreground there is a strong correlation between the residual value of  $C(0)$  and the Galactic latitude:  $C(0) \propto (\sin |b|)^{-\alpha}$  with  $\alpha \simeq 2$ . From least square fits we found  $\alpha = 2.2, 2.4, 2.5$  and  $1.7$  for 1.25, 2.2, 3.5, and 4.9  $\mu\text{m}$  respectively. At longer wavelengths the correlation with  $b$  is significantly less pronounced due to appreciable contributions from the zodiacal foreground. At short wavelengths (1.25 - 4.9  $\mu\text{m}$ ) the remaining fluctuations are still mainly due to point sources, which are recognizable as small groups of bright pixels in the original maps. This is confirmed by inspection of the histograms of the pixel brightnesses, which are asymmetric as expected for a distribution of point sources at various distances (Paper I, Fig. 5). Because point sources clearly dominate the fluctuations, the choice of  $N_{\text{cut}}$  is important in the near-IR. On the other hand, removal of large scale gradients using a variety of polynomial fits after

removing point sources makes little difference to the calculation of  $C(0)$  for these bands.

At longer wavelengths the situation is quite different. The sky brightness is dominated in most directions outside the Galactic Plane by the interplanetary dust, which is very smoothly distributed except for a cusp in the Ecliptic plane and some faint dust bands within a few degrees of it. There are also clouds of dust grains in resonance with the Earth's orbit, which appear in the Ecliptic plane  $90^\circ$  from the Sun (Reach *et al.* 1995b). Outside these regions, the main foreground structures are interstellar dust, which has typical size scales larger than the DIRBE beam ( Waller and Boulanger, 1994; Low and Cutri, 1994). Therefore it makes a difference whether large scale gradients are removed before computation of  $C(0)$ . The distribution of pixel brightnesses is also more nearly Gaussian and much less asymmetrical than at short wavelengths, and the choice of the desouring parameter  $N_{\text{cut}}$  makes little difference.

Because the measured fluctuations in the mid-IR are so small relative to the total brightness, and point sources are not the obvious source of fluctuations, we must evaluate instrument noise effects. Inspection of the raw data shows that the detector noise is comparable to the digitization roundoff noise for each detector sample except in Bands 9 and 10 where the detector noise dominates. The onboard phase sensitive detection algorithm obtains 8 digital samples per chopper cycle of the analog preamplifier outputs. The DIRBE beam scan rate is such that four of these chopper cycles are averaged to obtain a single photometric measure of the sky brightness at each pixel location. The rms conversion noise is  $12^{-0.5}$  digital units per sample, so that for a single pixel measurement consisting of 32 digital values, one obtains an rms digital noise of 0.051 digital units. The preamplifier gain is 16 for the sky observations, so that the conversion of the digital units to photometric units yields digitization noise levels of  $3.2$ ,  $1.7$ , and  $0.4$   $\text{nWm}^{-2}\text{sr}^{-1}$  in the J, K and L bands,  $0.6$  -  $0.9$   $\text{nWm}^{-2}\text{sr}^{-1}$  for the bands between  $4.9$  and  $100$   $\mu\text{m}$  , and

1.7-5.6  $\text{nWm}^{-2}\text{sr}^{-1}$  in the 140 and 24  $\mu\text{m}$  bands. These digitization noise estimates are further reduced by a factor of 17 by averaging the individual photometric measures for each pixel, since each pixel is observed about 15 times per week, and 20 weeks per year. Regions near the ecliptic poles are observed substantially more frequently. During this time the brightness of the interplanetary dust changes dramatically because of the Earth’s motion through the dust cloud, so wide ranges of the digitizer are exercised. Therefore the digitization errors are randomized so that they do not introduce obvious band structures in the completed annual map. We verified this from an average map made without subtracting a model for the interplanetary dust.

On the other hand, we make a separate correction for the interplanetary dust contribution for each weekly map. Systematic errors in the corrections can produce artificial stripes in the computed average map, which are seen most easily in the Ecliptic plane where the signals and their rates of change are greatest. These stripes have not been entirely eliminated by the dust model we used, and are one reason why the  $C(0)$  maps show increases near the Ecliptic plane even though the dust emission is expected to be very smooth. These stripes have least effect at the Ecliptic poles.

We conclude that the measured values for the fluctuations are upper limits on the fluctuations of the CIB. The upper limits estimated below come from the quietest patch in each band for the entire sky. For brevity we omit the histogram distribution of  $C(0)$ , but its inspection shows that the minimum is estimated from around 30-80 patches in each of the bands making it a reliable and unbiased estimate of the true upper limit. Since the distribution of  $C(0)$  is highly anisotropic on the sky, the signal must come from the foreground emission and it is thus further unlikely that any of the truly cosmological contributions have been removed in the process. Plate 1 shows that the lowest  $C(0)$  for the adjacent bands come from neighbouring patches. In the near IR these are located around

Galactic poles; in the mid-IR they are near Ecliptic poles and in the far-IR they shift back to the Galactic poles. Our data processing does not remove real fluctuations unless they appear to come from point sources, or to have very large scale gradients. The instrument digitization noise, estimated to be below  $1.0 \text{ nWm}^{-2}\text{sr}^{-1}$  in all bands after averaging, is not a problem at the level probed here.

#### 4. Results and conclusions

The measured upper limits on the fluctuations of the CIB offer a powerful test of any model for its sources. Fig. 2 summarizes our results at all except the two longest wavelength DIRBE bands. Triangles show the upper limits we set on  $\sqrt{C(0)}$ . These upper limits were calculated by selecting the sky patch with the lowest value of  $C(0)$  from among the ensemble of 384 patches. Translating these into limits on the uniform part of the CIB is somewhat theory-dependent. Assuming typically 10% fluctuations on the scale of the DIRBE beam, our results lead to quite low upper limits on the CIB fluxes from clustered material, particularly at mid- to far-IR bands. They are less interesting at 140 and 240  $\mu\text{m}$  because of higher DIRBE detector noise. The darkest DIRBE sky limits from weekly maps are presented with  $\times$ -s as reported by DIRBE (Hauser 1993). (A typical pixel is observed for 20 weeks during the mission). The vertical bars show the residual fluxes from the fits reported by Hauser (1996a) after removal of Galactic and zodiacal foregrounds, but they were not described as detections because of uncertainties in the foreground modeling.

At wavelengths  $>10\mu\text{m}$  they are comparable to the levels that may be derived from the interpretation of the spectra of  $\gamma$ -ray sources, where gamma rays interact with the CIB by pair production. One method of calculation gives the result as  $\nu I_\nu \simeq 6h(\frac{\lambda}{\mu\text{m}})^{0.55} \text{nWm}^{-2}\text{sr}^{-1}$  (Dwek and Slavin 1994), plotted with solid lines for  $h=H_0/100\text{kmsec}^{-1}\text{Mpc}^{-1}=1$  (upper line) and 0.5. If these are treated as detections our upper limits on  $C(0)$  would suggest that

the bulk of the CIB at these wavelengths is produced at very high  $z$ , leading to the decrease of  $(\nu I_\nu)_{z,rms}$  for given  $\nu I_\nu$ . In other words this would require  $\delta I/I \leq 2 \times 10^{-2} h^{-1} (\frac{\lambda}{40\mu\text{m}})^{-0.55}$ , so the background must come from high redshifts. An alternative interpretation would be that the CIB estimated from the  $\gamma$ -rays is not produced by clustered material. The latter is however unlikely since the CIB is expected to be produced by material that collapsed due to local gravity, and hence its structure should reflect that of the primordial density field.

At the J, K, L (1.25 - 3.5  $\mu\text{m}$ ) bands the no-evolution (Paper I) or reasonable evolution (Veeraraghavan 1996) models of the zero lag correlation function in the CIB produced by normal galaxies give numbers for  $\sqrt{C(0)}$  around (1.5-3, 0.5-1.5, 0.5-1.5)  $\text{nW m}^{-2} \text{sr}^{-1}$  respectively. Our limits at 1.25  $\mu\text{m}$  are almost an order of magnitude higher, but at 2.2 and 3.5  $\mu\text{m}$  they are comparable in magnitude. If there were an extra population of galaxies at early times they would contribute an additional signal (see e.g. the Cole, Treyer and Silk (1992) model designed to fit simultaneously the deep K- and B-counts). Any other sources of emission that may have been active in the early Universe in addition to normal galaxies would increase the above theoretical estimates.

Further improvements in the analysis of the DIRBE maps are possible, as are new instruments or new applications of old instruments. They may yield the first clear sign of a cosmic infrared background radiation.

We are grateful to Carlton Baugh for providing us with the APM power spectrum data, and to Michael Hauser for a careful reading of an early draft of this paper. This work was supported by NASA Long Term Space Astrophysics grant. The DIRBE software team developed the data sets and the software used for removing sources and interplanetary dust models. The National Aeronautics and Space Administration/Goddard Space Flight Center (NASA/GSFC) is responsible for the design, development, and operation of the Cosmic Background Explorer (COBE). GSFC is also responsible for the development of the analysis

software and for the production of the mission data sets. The COBE program is supported by the Astrophysics Division of NASA's Office of Space Science and Applications.

## References

Baugh, C.M. and Efstathiou, G. 1993, MNRAS, **265**, 145.

Beichman, C.A. and Helou, G. 1991, Ap.J., **370**, L1.

Bennett, C.L. *et al.* 1996, Ap.J., accepted.

Bernard, J.P. *et al.* 1994, A&A, **291**, L5.

Boggess, N.W. *et al.* 1992, Ap.J., **397**, 420.

Bond, J.R. *et al.* 1986, Ap.J., **306**, 428.

Bond, J.R. *et al.* 1991, Ap.J., **367**, 420.

COBE 1995a, COBE Skymap Information, National Space Sciences Data Center,  
[http://www.gsfc.nasa.gov/astro/cobe/skymap\\_info.html](http://www.gsfc.nasa.gov/astro/cobe/skymap_info.html)

COBE 1995b, DIRBE Explanatory Supplement, eds. M.G. Hauser, T. Kelsall, D. Leisawitz, and J. Weiland, National Space Sciences Data Center, anonymous FTP from nssdca.gsfc.nasa.gov.

Cole, S., Treyer, M. and Silk, J. 1992, Ap.J., **385**, 9.

Chan, F.K. and O'Neill 1975, Computer Sciences Corporation EPRF Report 2-75.

Chan, F.K. and Laubscher, R.E. 1976, Computer Sciences Corporation EPRF Report 3-76.

Dwek, E. and Slavin, J. 1994, Ap.J., **436**, 696.

Franceschini, A. *et al.* 1991, Ap.J.Suppl., **89**, 285.

Gunn, J. 1965, Ph.D. Thesis, Caltech. (unpublished)

Hauser, M. *et al.* , 1984, Ap.J. (Letters), **278**, L15.

Hauser, M. 1993, in “Back to the Galaxy,” AIP Conf. Proc. **278**, eds. S. Holt and F. Verter, (AIP:NY), 201.

Hauser, M. 1996a, in Proc. IAU Symposium 168, “Examining the Big Bang and Diffuse Background Radiations”, M. Kafatos and Y. Kondo, eds., Kluwer, Dordrecht., p. 99.

Hauser, M. 1996b, in “Unveiling the Cosmic Infrared Background,” AIP Conf. Proc., **348**, ed. E. Dwek, (AIP:NY), 11-24.

Kashlinsky, A. 1992, Ap.J., **399**, L1.

Kashlinsky, A., Mather, J., Odenwald, S. and Hauser, M. 1996, Ap.J., accepted (Paper I)

Koo, D. and Kron, R.R. 1992, ARAA, **30**, 613.

Low, F.J and Cutri, R.M. 1994, IR Physics and Tech. 35, 291.

Maddox, S. *et al.* 1990, MNRAS, **242**, 43P.

Martin, C. and Bowyer, S. 1989, Ap.J, **338**, 677.

Pagel, B.E.J. 1993, in “The Cold Universe,” eds. Montmerle *et al.*, Editions Frontieres, p.345

Peebles, P.J.E. 1980, “Large Scale Structure of the Universe,” Princeton Univ. Press.

Reach, W. *et al.* , 1995b, Nature, TBD, TBD.

Reach, W. *et al.* , 1996, in “Unveiling the Cosmic Infrared Background,” 1996, AIP Conf. Proc., **348**, (AIP: New York), 37-46.

Veeraraghavan, S. 1996, in “Unveiling the Cosmic Infrared Background,” AIP Conf. Proc, **348**, (AIP: New York), 122-126.

Waller, W. and Boulanger, F. 1994, ASP Conference Series, v. 58, 129.

Wang, B. 1991, Ap.J., **374**, 465.

Weiland, J.L. *et al.* , 1996, in “Unveiling the Cosmic Infrared Background,” AIP Conf. Proc. **348**, (AIP: New York), 74-80.

White, R.A., and Mather, J.C. 1991, “Databases from the Cosmic Background Explorer (COBE),” Databases & On-line Data in Astronomy. Astrophysics and Space Science Library, eds. M.A. Albrecht and D. Egret, (Dordrecht: Kluwer), 171, pp. 30-34.

### Figure captions

Fig. 1.  $A_\vartheta(z)$  is plotted vs  $z$  for 1) zero cosmological constant with  $\Omega=1$  (uppermost curves) and  $\Omega=0.1$  (lowermost curves) and 2) flat Universe with  $\Omega = 0.1$  and non-zero cosmological constant (middle curves). Dashed lines correspond to the APM fit spectrum from K92 and solid lines to BE. Three sets of each line correspond to one-sigma uncertainty in the BE fit and approximately the same uncertainty for K92.

Fig. 2. Triangles show the upper limits on  $\sqrt{C(0)}$  set by our analysis.  $\times$ -s are the lowest upper limits from the darkest part of the DIRBE weekly sky maps from (Hauser 1993). Vertical bars show the range of the residual DIRBE fluxes left after Galaxy modelling and removal (Hauser 1996a,b). Solid lines are the possible detections from Dwek and Slavin (1994); the upper line is for  $H_0=100$  km/sec/Mpc and the lower one is for 50km/sec/Mpc. All fluxes are in  $\text{Wm}^{-2}\text{sr}^{-1}$ .

Plate 1. Maps of  $C(0)$  in Galactic coordinates for DIRBE Bands 1-8, 1.25 - 100  $\mu\text{m}$ . The grey scale shows logarithmic steps at intervals of 1.8. For Bands 1-8, the minimum  $\log(C(0))$  are -4.2, -4.7, -5.1, -5.4, -6.0, -4.1, -3.3 and -2.5 respectively.

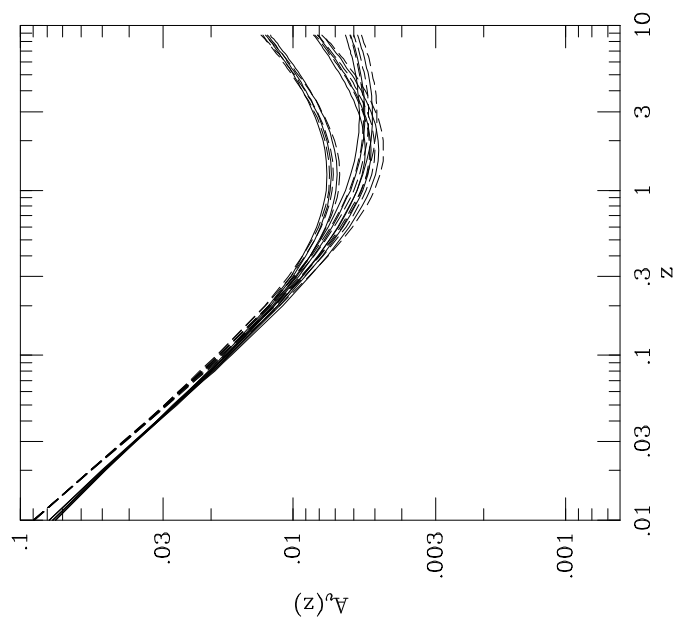


Fig. 1.—

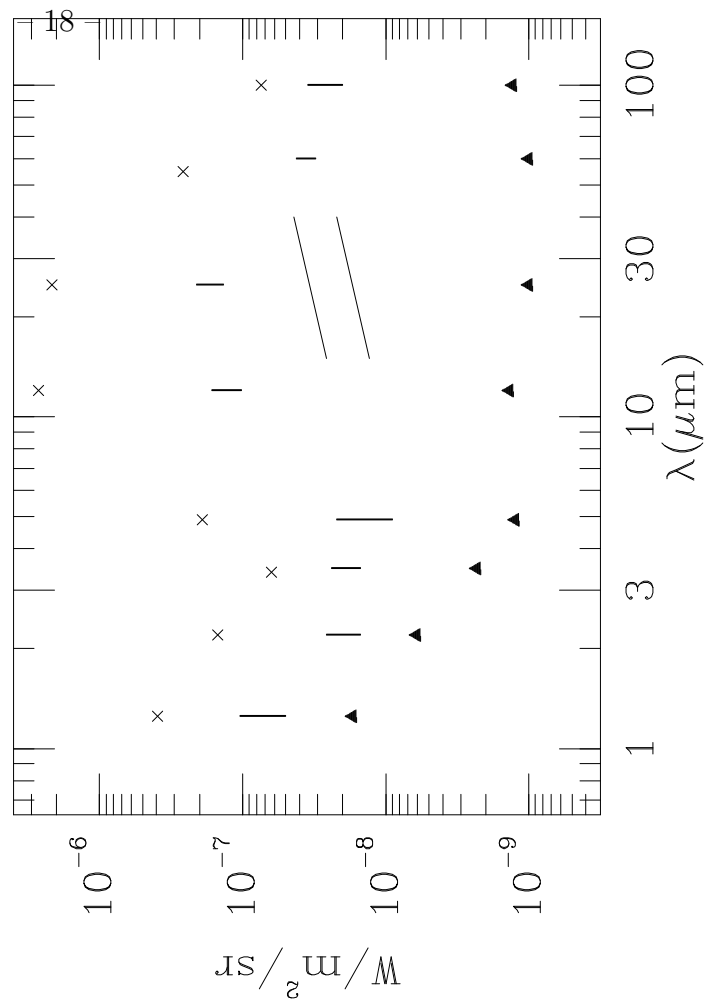
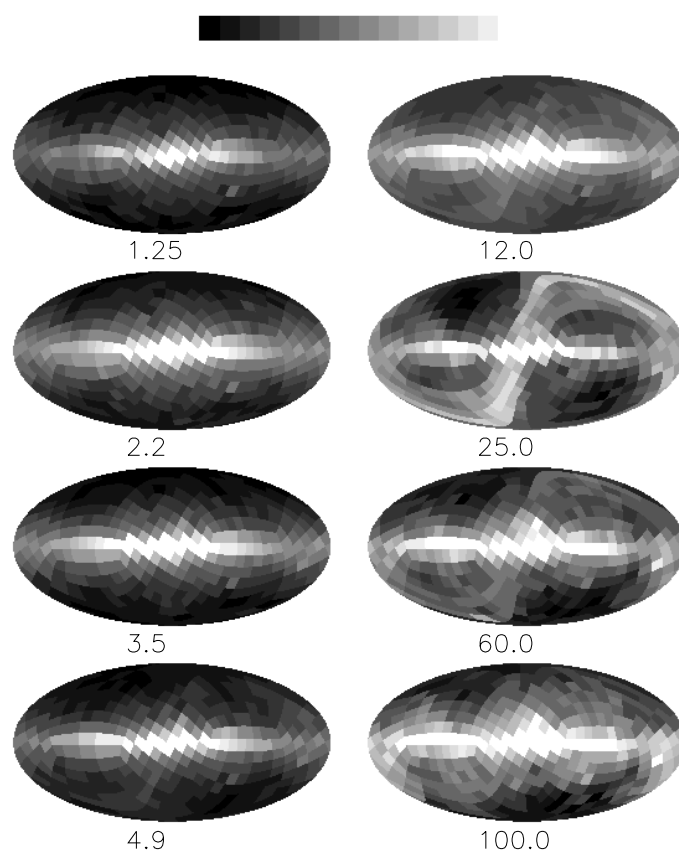


Fig. 2.—



**Plate 1.**